EARTHQUAKE ENGINEERING AND STRUCTURAL DYNAMICS
Earthquake Engng. Struct. Dyn. **28**, 61–77 (1999)

SYSTEM IDENTIFICATION OF LINEAR MDOF STRUCTURES UNDER AMBIENT EXCITATION

SER TONG QUEK*,†, WENPING WANG‡ AND CHAN GHEE KOH†
Department of Civil Engineering, National University of Singapore, 10 Kent Ridge Crescent, Singapore 119260, Singapore

SUMMARY

This paper introduces the eigenspace structural identification technique for tall buildings subjected to ambient excitations that are stationary and where only the response time histories are measured. Based on the forward innovation model of the Kalman filter sequence, the actual response can be constructed as a function of the measured response time history with contamination of either displacement or velocity. The response time history is decomposed into subspace matrices using QR decomposition and Quotient Singular Value Decomposition (QSVD) techniques. These are then substituted into the least-square formulation to obtain the solution which is non-unique. Similarity transformation is applied to arrive at the desired solution employing the fact that eigenvalues of self-similar systems are identical. The advantages of this eigenspace technique are that it is non-iterative, initial estimates of the parameters to the identified are not required, well-established numerical algorithm of the decomposition techniques employed are available, and the method can handle MDOF systems efficiently. Copyright © 1999 John Wiley & Sons, Ltd.

KEY WORDS: system identification; tall buildings; ambient vibration; stochastic model; band limited excitation; eigenspace algorithm

INTRODUCTION

System Identification (SI) techniques to study the actual states of civil engineering structures have received considerable attention in recent years, as extensive full-scale experimental studies are expensive and often difficult to perform. The approaches in SI techniques can be classified under time domain and frequency domain. The simplest solution in the time-domain approach is by the method of least squares.[1–3] For cases in which the measurements are contaminated with noise, the least-squares algorithm can give biased results.[4] This problem has been addressed by methods such as Instrumental Variable,[5] Maximum Likelihood[6,7] and Extended Kalman Filter or EKF.[8–10] These methods are often iterative in nature and the quality of the results dependent on the initial estimates of the parameters to be identified. The convergence for problems with numerous degrees of freedom (DOF) cannot be always guaranteed.

* Correspondence to: Ser Tong Quek, Department of Civil Engineering, National University of Singapore, 10 Kent Ridge Crescent, Singapore 119260. E-mail: cveqst@nus.edu.sg
† Associate Professor
‡ Research Scholar

CCC 0098–8847/99/010061–17$17·50

Received 22 August 1997
Revised 12 May 1998

In practice, records of the input excitation are not always available. They are either not measured, as in most cases of ambient vibration, or the data obtained are highly corrupted and hence unusable. Torkamani and Ahmadi[11] estimated the stiffness coefficients for an 18-storey building by extracting the mode shapes and frequencies of the structure from the response data under ambient excitation, based on Fourier analysis technique. However, damping is not considered. Ambient excitation, such as that caused by wind, can be approximated as ergodic and stationary band-limited Gaussian white noise processes.[12,13] Wang and Halder[14] modelled the unknown input as such and used the Generalized Least-Squares (GLS) method to estimate the structural parameters. However, the convergence of GLS is often dependent on the order in which the noise excitations are modelled.[15] Alternatively, Jones *et al.*[16] used the Kalman filter technique to identify the parameters as well as the input excitation. These methods again require reasonable initial estimates of the parameters, and often limited to problems with few DOFs.

The Eigenspace Algorithm (EA) is introduced to overcome both deficiencies for identification of structures with unknown input excitation. The original form was first proposed by Van Overschee and De Moor[17] for discrete-time state-space model, and is adapted in this paper for continuous-time model by introducing an Observable Canonical Form (OCF) and the corresponding similarity transformation. A somewhat similar approach was taken by the Eigensystem Realization Algorithm[18] (ERA) which utilized the uniqueness of the eigenvalues to identify the parameters and employed the Singular Value Decomposition (SVD) in the numerical solution. However, for large systems or long data series, the ERA can be cumbersome and the Quotient Singular Value Decomposition (QSVD) is proposed in EA to overcome this problem. The EA can handle measured responses in terms of either displacement or velocity. The advantages of EA are that (a) no initial estimates of the parameters to be identified are required, (b) it is non-iterative and hence has no convergence problem, and (c) the QR decomposition and QSVD required in the solution process are well developed and efficient. The algorithm is purely data driven and the non-linear computation of noise covariance as in EKF technique can be avoided. Numerical examples involving the identification of tall buildings under ambient vibration are given in this paper to illustrate the efficiency and accuracy of EA with respect to the length as well as noise of measured responses and the bandwidth of the actual input excitation. Both displacement and velocity response data are considered.

MATHEMATICAL FORMULATION

Consider a structure idealized as a lumped mass system with m degrees of freedom subjected to an unknown band-limited excitation, which is modelled as a pure white noise $u(t)$ passing through a filter J. The horizontal equation of motion can be written as

$$M\ddot{q}(t) + C\dot{q}(t) + Kq(t) = Ju(t) \tag{1}$$

where M, C and K are the mass, damping and stiffness matrices of the structure, respectively, q is a $(m \times 1)$ dimensional vector of the resulting lateral structural displacements, and the overdot denotes differentiation with respect to time t. The equation of motion and the measured displacement can be written in the state-space form as

$$\begin{aligned} \dot{x}(t) &= F_c x(t) + H_c u(t) \\ y(t) &= D_c x(t) + v(t) \end{aligned} \tag{2}$$

where

$$x(t) = \begin{pmatrix} q(t) \\ \dot{q}(t) \end{pmatrix}, \qquad F_c = \begin{bmatrix} 0_{m\times m} & I_{m\times m} \\ -M^{-1}K & -M^{-1}C \end{bmatrix}, \qquad H_c = \begin{bmatrix} 0_{m\times m} \\ M^{-1}J \end{bmatrix}, \qquad D_c = [I_{m\times m}\, 0_{m\times m}] \quad (3)$$

in which $0_{m\times m}$ is a $m\times m$ null matrix, and $I_{m\times m}$ is a $m\times m$ identity matrix. The measured displacement $y(t)$ is assumed to be contaminated by Gaussian white noise $v(t)$. In this paper, equation (2) is defined as the Observable Canonical Form (OCF) of the state-space equation, and the matrices in OCF are denoted with a subscript c. That is, the two components F_c and D_c of the observability matrix are such that the matrix F_c is filled with $0_{m\times m}$ and $\mathrm{I}_{m\times m}$ in the upper half and the unknown parameters to be identified located in the lower part, and the matrix D_c comprises $\mathrm{I}_{m\times m}$ and $0_{m\times m}$. If the measured response is velocity instead of displacement, the continuous-time state-space equation can also be transformed into the OCF (see the appendix).

The continuous-time state-space form of equation (2) can be expressed in discrete-time form for the kth time step as

$$\begin{aligned} x_{k+1} &= Ax_k + Bu_k = Ax_k + w_k \\ y_k &= Dx_k + v_k \end{aligned} \quad (4)$$

with

$$A = \mathrm{e}^{F_c \Delta t} = \sum_{j=0}^{\infty} \frac{(F_c \Delta t)^j}{j!}, \qquad B = \int_0^{\Delta t} \mathrm{e}^{F_c \tau} H_c \, \mathrm{d}\tau = F_c^{-1}(A - I)H_c \quad (5)$$

where Δt denotes the size of each time step. Also, w_k and u_k in equation (4) are related by the covariance matrix $E(w_k w_l^{\mathrm{T}}) = BE(u_k u_l^{\mathrm{T}})B^{\mathrm{T}}$, where $E(.)$ denotes expectation. Note that the matrix D is the same as D_c of the continuous formulation.

For system identification to be possible, the system must be observable and controllable. That is, all the modes of the system must be represented in the output y_k, and all dynamical modes of the system are stable and excited by the process noise. The observability matrix O_i is defined as

$$O_i = \begin{bmatrix} D \\ DA \\ \vdots \\ DA^{i-1} \end{bmatrix} \quad (6)$$

which has rank $2m$.[19] The extended controllability matrix is given by

$$\Delta_i = [\mathrm{A}^{i-1} G \ \ldots \ AG \ G] \quad (7)$$

where $G = E(x_{k+1} y_k^{\mathrm{T}})$.

SIMILARITY TRANSFORMATION

For a given noise excitation and response data, the solution for A and D is non-unique. It takes the form $T^{-1}AT$ and DT, where T is any non-singular square matrix. However, the eigenvalues of A and $T^{-1}AT$ are identical.[19] If the forms of A and D are prescribed, as in the OCF of

equation (3), then the solution obtained can be transformed to this desired form through a transformation matrix T.

In the discrete-time state-space formulation, if A and D are the solution obtained, which in general is not in the OCF, the transformation matrix T_1 given by (see the appendix)

$$T_1 = \begin{bmatrix} D \\ DA \end{bmatrix}^{-1} \tag{8}$$

must be applied to obtain the OCF as follows:

$$A_c = T_1^{-1} A T_1, \quad B_c = T_1^{-1} B, \quad D_c = D T_1 \tag{9}$$

To obtain the continuous-time state-space solution, the matrix A_c in OCF is substituted in equation (5) to get the matrix F_c where the latter may not necessarily be in the OCF. Through similarity transformation, the desired solution can be computed as

$$F_c = T_2^{-1} \left[\frac{1}{\Delta t} \ln A_c \right] T_2, \quad T_2 = \begin{bmatrix} D_c \\ D_c \left[\frac{1}{\Delta t} \ln A_c \right] \end{bmatrix}^{-1} \tag{10}$$

By comparing with F_c in equations (3) and (10), sub-matrices $M^{-1}K$ and $M^{-1}C$ can be extracted. If M is known, K and C can be obtained by direct matrix multiplication.

EIGENSPACE ALGORITHM

The least-square solution to equation (4), assuming that both w_i and v_i are independent of x_i, can be written as

$$\begin{aligned} A &= E(x_{i+1} x_i^{\mathrm{T}}) E(x_i x_i^{\mathrm{T}})^{-1} \\ D &= E(y_i x_i^{\mathrm{T}}) E(x_i x_i^{\mathrm{T}})^{-1} \end{aligned} \tag{11}$$

The actual response x_i at time-step i can be written in terms of the measured response of the previous i time steps and the system matrices, based on the innovation model of the Kalman filter sequence. To convert the system matrices as functions of the measured response time history, the QR decomposition and QSVD algorithms are employed for extracting the relevant sub-matrices. These sub-matrices can be interpreted geometrically as eigenspace projections based solely on the response behaviour of the system.

It can be shown by Van Overschee and De Moor[17] that the measured response covariance matrix can be expressed as

$$\begin{aligned} \Lambda_i &= E[y_{k+i} y_k^{\mathrm{T}}] = D A^{i-1} G \\ \Lambda_{-i} &= G^{\mathrm{T}} [A^{i-1}]^{\mathrm{T}} D^{\mathrm{T}} \end{aligned} \tag{12}$$

where y_k denotes the measured response of the m DOFs at time-step k. For finite but sufficiently long records, say of j time steps, the actual computation of the matrix can be approximated by

$$\Lambda_i \approx \frac{1}{j} \sum_{k=0}^{j-1} y_{k+i} y_k^{\mathrm{T}} \tag{13}$$

Assume that the response measurements are taken for time-steps 0 to $2i+j-2$. An output Hankel matrix of $2i \times j$ blocks, where each block is of size $m \times 1$, can be formulated as

$$Y_{0|2i-1} = \begin{bmatrix} y_0 & y_1 & \cdots & y_{j-1} \\ y_1 & y_2 & \cdots & y_j \\ \vdots & \vdots & & \vdots \\ y_{2i-1} & y_{2i} & \cdots & y_{2i+j-2} \end{bmatrix} \tag{14}$$

where the first subscript in Y denotes the time step of the upper left element while the second subscript is the time step of the bottom left element. The matrix A to be identified has rank $2m$. Hence, the integers i and j must be larger than $2m$, to ensure that the rank of $Y_{0/i}$ will also be $2m$. The correlation between different output Hankel matrices can be written as

$$E_j[Y_{i|2i-1}\, Y_{0|i-1}^{\mathrm{T}}] = \begin{bmatrix} \Lambda_i & \Lambda_{i-1} & \cdots & \Lambda_1 \\ \Lambda_{i+1} & \Lambda_i & \cdots & \Lambda_2 \\ \vdots & \vdots & & \vdots \\ \Lambda_{2i-1} & \Lambda_{2i-2} & \cdots & \Lambda_i \end{bmatrix} = O_i \Delta_i \tag{15}$$

where the subscript j denotes the summation being taken over j time steps as in equation (13).

Based on the forward innovation model of the Kalman filter, the estimate of x_i can be written explicitly as

$$x_i = \Delta_i L_i^{-1} \begin{pmatrix} y_0 \\ y_1 \\ \vdots \\ y_{i-1} \end{pmatrix} \tag{16}$$

where L_i is defined as

$$L_i = \begin{bmatrix} \Lambda_0 & \Lambda_{-1} & \cdots & \Lambda_{1-i} \\ \Lambda_1 & \Lambda_0 & \cdots & \Lambda_{2-i} \\ \vdots & \vdots & & \vdots \\ \Lambda_{i-1} & \Lambda_{i-2} & \cdots & \Lambda_0 \end{bmatrix} = E_j[Y_{0|i-1}\, Y_{0|i-1}^{\mathrm{T}}] = E_j[Y_{i|2i-1}\, Y_{i|2i-1}^{\mathrm{T}}] \tag{17}$$

The proof by mathematical induction is given in Appendix A.2 of Reference 17. For j time steps, define $X_i = (x_i\, x_{i+1}\, \ldots\, x_{i+j-1})$ of size $2m \times j$. Equation (16), and equation (11) in view of the basis of equation (13), become

$$\begin{gathered} X_i = \Delta_i L_i^{-1} Y_{0|i-1} \\ A \approx E_j(X_{i+1} X_i^{\mathrm{T}})\, E_j(X_i X_i^{\mathrm{T}})^{-1} = (X_{i+1} X_i^{\mathrm{T}})(X_i X_i^{\mathrm{T}})^{-1} \\ D \approx E_j(Y_{i|i} X_i^{\mathrm{T}})\, E_j(X_i X_i^{\mathrm{T}})^{-1} = (Y_{i|i} X_i^{\mathrm{T}})(X_i X_i^{\mathrm{T}})^{-1} \end{gathered} \tag{18}$$

As X_i is a function of Δ_i which contains system parameters to be identified, it is thus necessary to find some way to express A and D in terms of the measured responses given in Y. For this purpose, QR decomposition and SVD of the eigenspace projection matrices are adopted.

By partitioning and performing QR decomposition on $Y_{0|2i-1}$ as

$$\begin{bmatrix} Y_{0|i-1} \\ Y_{i|2i-1} \end{bmatrix} = \begin{matrix} mi \\ mi \end{matrix} \overset{\begin{matrix} mi & mi \end{matrix}}{\begin{bmatrix} R_{11} & 0 \\ R_{21} & R_{22} \end{bmatrix}} \begin{bmatrix} Q_{0|i-1}^{\mathrm{T}} \\ Q_{i|2i-1}^{\mathrm{T}} \end{bmatrix} \tag{19}$$

where $Q_{0|i-1}^{T}$ and $Q_{i|2i-1}^{T}$ are orthogonal, the QSVD matrix pair can be obtained as

$$\begin{aligned} R_{21} &= Z_i S_i^{\mathrm{T}} U_i^{\mathrm{T}} \\ R_{22} &= Z_i T_i^{\mathrm{T}} V_i^{\mathrm{T}} \end{aligned} \tag{20}$$

Each of the matrices S_i and T_i contains only $2m$ non-zero elements arranged diagonally in descending order. The matrices U_i and V_i are orthonormal, in which only the first $2m$ columns are actually necessary for computation. The SVD of the matrix projection between $Y_{0|i-1}$ and $Y_{i|2i-1}$ can be written as[20]

$$\begin{aligned} &Y_{0|i-1}^{\mathrm{T}}(E_j[Y_{0|i-1}\, Y_{0|i-1}^{\mathrm{T}}])^{-1}(E_j[Y_{0|i-1}\, Y_{i|2i-1}^{\mathrm{T}}])(E_j[Y_{i|2i-1}\, Y_{i|2i-1}^{\mathrm{T}}])^{-1} Y_{i|2i-1} \\ &\quad = (Q_{0|i-1}\, U_i) S_i (Q_{0|i-1}\, U_i S_i + Q_{i|2i-1} V_i T_i)^{\mathrm{T}} \end{aligned} \tag{21}$$

Physically, the above equation is a projection of $Y_{0|i-1}$ onto the space spanned by $Y_{i|2i-1}$ and the result can be interpreted as an improved prediction of $Y_{0|i-1}$ whereby the noise component orthogonal to $Y_{i|2i-1}$ is removed. The Left-Hand Side (LHS) of equation (21), in view of equations (15), (17) and (18), can be expressed as

$$Y_{0|i-1}^{\mathrm{T}} L_i^{-1} \Delta_i^{\mathrm{T}} O_i^{\mathrm{T}} L_i^{-1} Y_{i|2i-1} = X_i^{\mathrm{T}} O_i^{\mathrm{T}} L_i^{-1} Y_{i|2i-1} \tag{22}$$

Comparing equations (21) and (22), let

$$\begin{aligned} X_i^{\mathrm{T}} &= Q_{0|i-1} U_i S_i^{1/2} \\ O_i^{\mathrm{T}} L_i^{-1} Y_{i|2i-1} &= S_i^{1/2} (Q_{0|i-1} U_i S_i + Q_{i|2i-1} V_i T_i)^{\mathrm{T}} \end{aligned} \tag{23}$$

It should be mentioned that the choice of X_I^{T} is only one possible realization and is therefore non-unique. However, the subsequent development of equations must be consistent with this choice in order to obtain meaningful results. The non-uniqueness is removed through similarity transformation. Based on equation (18), D can be identified as

$$\begin{aligned} D &= (Y_{i|i}\, X_i^{\mathrm{T}})(X_i\, X_i^{\mathrm{T}})^{-1} = [I_{m\times m}\, 0_{m\times m(i-1)}]\; Y_{i|2i-1}\, X_i^{\mathrm{T}} (X_i\, X_i^{\mathrm{T}})^{-1} \\ &= [I_{m\times m}\, 0_{m\times m(i-1)}]\, (Z_i S_i^{\mathrm{T}} U_i^{\mathrm{T}} Q_{0|i-1}^{\mathrm{T}} + Z_i T_i^{\mathrm{T}} V_i^{T} Q_{i|2i-1}^{\mathrm{T}})(Q_{0|i-1}\, U_i S_i^{1/2}) \\ &\quad \times [S_i^{1/2} U_i^{\mathrm{T}} Q_{0|i-1}^{\mathrm{T}} Q_{0|i-1} U_i S_i^{1/2}]^{-1} \\ &= [I_{m\times m}\, 0_{m\times m(i-1)}]\, Z_i S_i^{1/2} \end{aligned} \tag{24}$$

Similarly, by repartitioning $Y_{0|2i-1}$ and performing QR decomposition as

$$\begin{bmatrix} Y_{0|i} \\ Y_{i+1|2i-1} \end{bmatrix} = \begin{matrix} m(i+1) \\ m(i-1) \end{matrix} \overset{\begin{matrix} m(i+1) & m(i-1) \end{matrix}}{\begin{bmatrix} R'_{11} & 0 \\ R'_{21} & R'_{22} \end{bmatrix}} \begin{bmatrix} Q_{0|i}^{\mathrm{T}} \\ Q_{i+1|2i-1}^{\mathrm{T}} \end{bmatrix} \tag{25}$$

the QSVD matrix pair $R'_{21} = Z_{i-1} S_{i-1}^{\mathrm{T}} U_{i-1}^{\mathrm{T}}$ and $R'_{22} = Z_{i-1} T_{i-1}^{\mathrm{T}} V_{i-1}^{\mathrm{T}}$ are obtained. The SVD of the matrix projection between $Y_{0/i}$ and $Y_{i+1/2i-1}$ can be written as

$$\begin{aligned} &Y_{0|i}^{\mathrm{T}}(E_j[Y_{0|i}\, Y_{0|i}^{\mathrm{T}}])^{-1}(E_j[Y_{0|i}\, Y_{i+1|2i-1}^{\mathrm{T}}])(E_j[Y_{i+1|2i-1}\, Y_{i+1|2i-1}^{\mathrm{T}}])^{-1}\, Y_{i+1|2i-1} \\ &\quad = (Q_{0|i} U_{i-1}) S_{i-1} (Q_{0|i} U_{i-1} S_{i-1} + Q_{i+1|2i-1} V_{i-1}\, T_{i-1})^{\mathrm{T}} \end{aligned} \tag{26}$$

As in equation (22), the LHS of equation (26) can be written as

$$Y_{0|i}^{\mathrm{T}} L_{i+1}^{-1} \Delta_{i+1}^{\mathrm{T}} O_{i-1}^{\mathrm{T}} L_{i-1}^{-1}\, Y_{i+1|2i-1} = X_{i+1}^{\mathrm{T}} O_{i-1}^{\mathrm{T}} L_{i-1}^{-1}\, Y_{i+1|2i-1} \tag{27}$$

Assuming that the observed data to be sufficiently long and the system to be stable, the projection of equations (21) and (26), which are based on exactly the same response time history, must be consistent. Specifically, the two SVDs must give consistent direction. Hence by introducing a scaling matrix M (of the same size as S_{i-1}) to account for the difference in the magnitude of the space vector, the following relationship must hold, namely:

$$X_{i+1}^{\mathrm{T}} = Q_{0|i} U_{i-1} S_{i-1}^{1/2} M^{\mathrm{T}} \tag{28}$$

To compute M, the relationship for long and stable records, i.e. time-steps j sufficiently large,

$$(Y_{i|2i-2}\, X_i^{\mathrm{T}})(X_i\, X_i^{\mathrm{T}})^{-1} = (Y_{i+1|2i-1}\, X_{i+1}^{\mathrm{T}})(X_{i+1}\, X_{i+1}^{\mathrm{T}})^{-1} \tag{29}$$

is employed. The LHS of equation (29) can be rewritten in the same manner as equation (24) as

$$\begin{aligned} (Y_{i|2i-2}\, X_i^{\mathrm{T}})(X_i\, X_i^{\mathrm{T}})^{-1} &= [I_{m(i-1)\times m(i-1)}\, 0_{m(i-1)\times m}]\; Y_{i|2i-1}\, X_i^{\mathrm{T}} (X_i\, X_i^{\mathrm{T}})^{-1} \\ &= [I_{m(i-1)\times m(i-1)}\, 0_{m(i-1)\times m}]\; Z_i S_i^{1/2} \end{aligned} \tag{30}$$

The RHS of equation (29), in view of equations (25) and (28), can be simplified as

$$\begin{aligned} Y_{i+1|2i-1}\, X_{i+1}^{\mathrm{T}} (X_{i+1}\, X_{i+1}^{\mathrm{T}})^{-1} &= (Z_{i-1} S_{i-1}^{\mathrm{T}} U_{i-1}^{\mathrm{T}} Q_{0|i}^{\mathrm{T}} + Z_{i-1} T_{i-1}^{\mathrm{T}} V_{i-1}^{\mathrm{T}} Q_{i+1|2i-1}^{\mathrm{T}}) \\ &\quad \times (Q_{0|i} U_{i-1} S_{i-1}^{1/2} M^{\mathrm{T}})[M (S_{i-1}^{1/2})^{\mathrm{T}} U_{i-1}^{\mathrm{T}} Q_{0|i}^{\mathrm{T}} Q_{0|i} U_{i-1} S_{i-1}^{1/2} M^{\mathrm{T}}]^{-1} \\ &= Z_{i-1} S_{i-1}^{1/2} M^{-1} \end{aligned} \tag{31}$$

From equations (30) and (31), M can be computed as

$$M = S_i^{-1/2} [[I_{m(i-1)\times m(i-1)}\, 0_{m(i-1)\times m}]\;\; Z_i]^{+}\, Z_{i-1}\, S_{i-1}^{1/2} \tag{32}$$

where the superscript + denotes the pseudo-inverse.

The identification of A using equation (18) can now be performed in terms of the decomposed matrices based on the response time history Y as

$$\begin{aligned} A = (X_{i+1}\, X_i^{\mathrm{T}})(X_i\, X_i^{\mathrm{T}})^{-1} &= M (S_{i-1}^{1/2} U_{i-1}^{\mathrm{T}} Q_{0|i}^{\mathrm{T}})(Q_{0|i-1} U_i S_i^{1/2})(S_i^{1/2} U_i^{\mathrm{T}} Q_{0|i-1}^{\mathrm{T}} Q_{0|i-1} U_i S_i^{-1/2})^{-1} \\ &= M\, S_{i-1}^{1/2} U_{i-1}^{\mathrm{T}} \begin{bmatrix} I_{m(i-1)\times m(i-1)} \\ 0_{m\times m(i-1)} \end{bmatrix} U_i S_i^{-1/2} \end{aligned} \tag{33}$$

NUMERICAL EXAMPLES

Example 1

A six-storey shear building[9] shown in Figure 1 is used where the lumped mass at each storey, m_i, is assumed to be known and the damping, c_i, and stiffness, k_i, are the system parameters to be identified. The known masses are 75, 65, 65, 60, 75 and 80, respectively from the lowest storey. The actual values of c_i and k_i to be compared with are given in Table I. The six natural frequencies of the structure are 4·25, 12·1, 19·2, 24·9, 30·2 and 34·2 rad/s. For verification purposes, the response time histories for identification are obtained using simulated data. Six independent band-limited white noise time histories are generated at a rate of 200 samples/s for each storey to simulate ambient excitation. Different duration of response time histories, at 10, 25, 40 and 50 s

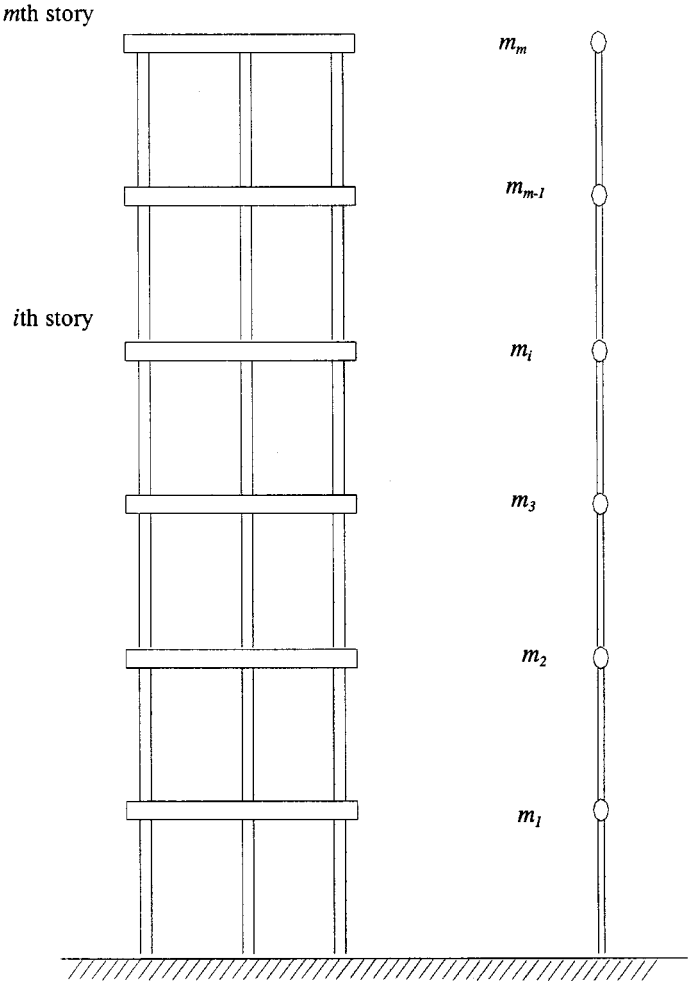

Figure 1. Structural model of m degree of freedom building

Table I. Effect of sampling length of response data (1 per cent noise added) on k and c using input excitation with frequency band 0–50 Hz based on displacement observation

Parameters	Stiffness, k				Damping, c			
Storey no.	Actual value	Mean predicted	cov	Per cent error in mean	Actual value	Mean predicted	cov	Per cent error in mean
Record length = 2000								
1	24 000	25 397	0·144	5·82	550	722·7	0·449	31·40
2	22 000	23 373	0·138	6·24	850	924·7	0·289	8·79
3	21 000	23 397	0·201	11·41	450	438·5	0·411	−2·56
4	19 500	20 365	0·171	4·44	500	579·2	0·249	15·84
5	18 000	18 065	0·151	0·36	650	671·8	0·514	3·35
6	16 000	15 873	0·185	−0·79	550	525·6	0·269	−4·44
Average of absolute values			0·165	4·84	—	—	0·364	11·06
Record length = 5000								
1	24 000	24 179	0·155	0·75	550	500·9	0·296	−8·93
2	22 000	23 507	0·099	6·85	850	888·5	0·117	4·53
3	21 000	21 820	0·097	3·90	450	412·1	0·170	−8·42
4	19 500	19 669	0·121	0·87	500	532·9	0·127	6·58
5	18 000	18 185	0·108	1·03	650	586·1	0·215	−9·83
6	16 000	16 723	0·117	4·52	550	548·8	0·237	−0·22
Average of absolute values			0·116	2·99	—	—	0·194	6·42
Record length = 8000								
1	24 000	25 332	0·071	5·55	550	564·9	0·194	2·71
2	22 000	21 601	0·049	−1·81	850	846·1	0·089	−0·46
3	21 000	21 412	0·052	1·96	450	441·6	0·166	−1·87
4	19 500	19 469	0·067	−0·16	500	528·4	0·172	5·68
5	18 000	18 913	0·107	5·07	650	691·3	0·145	6·35
6	16 000	16 383	0·103	2·39	550	533·8	0·229	−2·95
Average of absolute values			0·075	2·83	—	—	0·166	3·34
Record length = 10 000								
1	24 000	24 369	0·066	1·54	550	507·1	0·143	−7·80
2	22 000	21 204	0·050	−3·62	850	813·5	0·085	−4·29
3	21 000	21 592	0·038	2·82	450	458·2	0·124	1·82
4	19 500	19 723	0·038	1·14	500	488·2	0·073	−2·36
5	18 000	17 949	0·098	−0·28	650	648·1	0·121	−0·29
6	16 000	16 555	0·080	3·47	550	565·8	0·140	2·87
Average of absolute values			0·062	2·15	—	—	0·114	3·24

corresponding to 2000, 5000, 8000 and 10 000 sampling points, are considered. The effect of the frequency bandwidth of input excitation is studied using input bandwidths of 10, 25, 50 and 75 Hz. As actual observation are contaminated with noise in practice, the effect of such noises on the identification results are investigated by numerically superimposing noise at 1, 3 and 5 per cent levels of root-of-mean-square (RMS) values of the time-integrated response, the latter obtained using the Runge–Kutta method. The identification results presented are the mean and coefficient of variation (cov) of c_i and k_i based on 10 time histories generated for each case. For the case of 10 000 sampling length, Figure 2 shows a typical input spectrum of bandwidth 0–50 Hz

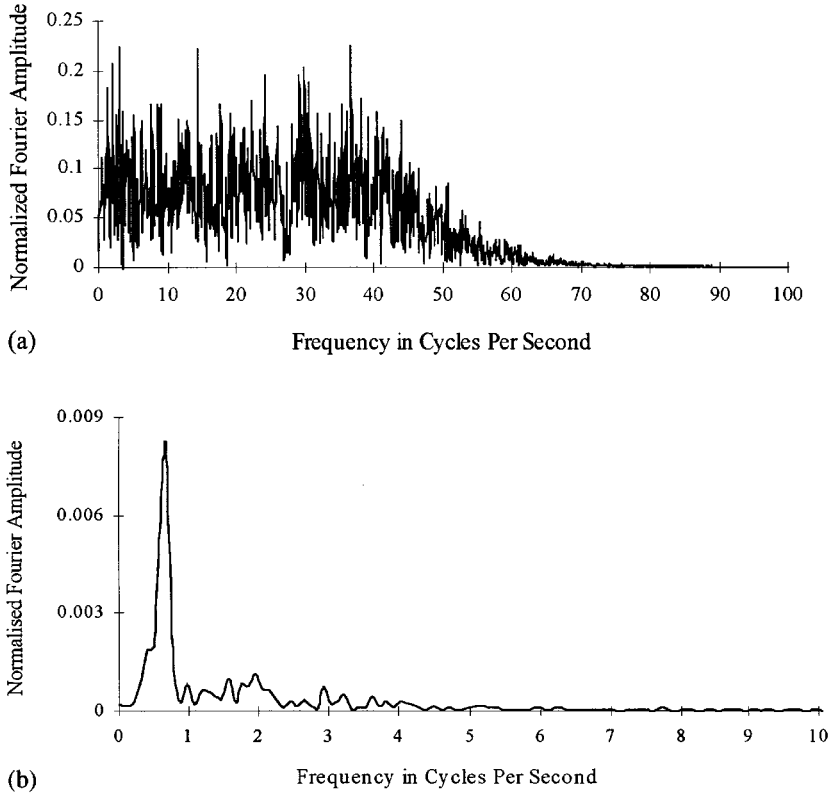

Figure 2. (a) Fourier amplitude spectrum of input excitation (0–50 Hz); (b) Fourier amplitude spectrum of storey displacement response

and the corresponding displacement response spectrum of the first storey. It is normalized by the data length such that a unit sinusoid in the time domain corresponds to unit amplitude in the frequency domain.

As can be seen from Table I, a record length of 2000 sampling points with 1 per cent noise added and input frequency bandwidth of 50 Hz produces mean error of 5 and 11 per cent and mean cov of 0·17 and 0·36 for k and c, respectively. The respective maximum values for k are 11·4 per cent and 0·20 and for c are 31·4 per cent and 0·51. As expected, with increase in sampling length the results for both k and c improve. For a record length of 10 000 sampling points, the mean error and cov for k, respectively, are 2 per cent and 0·06. The corresponding values for c are 3 per cent and 0·11. The respective maximum values for k are 3·6 per cent and 0·10 and for c are 7·8 per cent and 0·14. For all cases, the prediction for k is better than for c, since parameter k is coupled with displacement in the equation. On the other hand, the prediction for c is better than for k, if the observation is given as velocity data.

In view of the fact that any input excitation that spans beyond the highest structural frequency range will be able to excite all the structural modes, it is important in structural identification that this condition be fulfilled to produce reasonable results. However, for input excitation bandwidth

Table II. Effect of bandwidth of input excitation on k and c for response data with 1 per cent noise and sampling length of 10 000 points based on displacement observation

Parameters	Stiffness, k				Damping, c			
Storey no.	Actual value	Mean predicted	cov	Per cent error in mean	Actual value	Mean predicted	cov	Per cent error in mean
Band width = 0–10 Hz								
1	24 000	22 283	0·090	−7·15	550	370·9	0·396	−32·56
2	22 000	20 703	0·090	−5·90	850	762·6	0·139	−10·28
3	21 000	19 685	0·105	−6·26	450	392·1	0·168	−12·87
4	19 500	20 546	0·169	5·36	500	551·8	0·329	10·36
5	18 000	21 245	0·252	18·03	650	846·2	0·366	30·18
6	16 000	17 320	0·186	8·25	550	608·9	0·311	10·71
Average of absolute values			0·149	8·49	—	—	0·285	17·83
Band width = 0–25 Hz								
1	24 000	25 087	0·099	4·53	550	457·8	0·186	−16·76
2	22 000	22 710	0·054	3·23	850	734·1	0·063	−13·64
3	21 000	21 850	0·024	4·05	450	382·0	0·071	−15·11
4	19 500	19 946	0·053	2·29	500	436·4	0·087	−12·72
5	18 000	19 163	0·048	6·46	650	541·1	0·061	−16·75
6	16 000	16 699	0·036	4·37	550	505·3	0·044	−8·13
Average of absolute values			0·052	4·15	—	—	0·085	13·85
Band width = 0–50 Hz								
1	24 000	24 369	0·066	1·54	550	507·1	0·143	−7·80
2	22 000	21 204	0·050	−3·62	850	813·5	0·085	−4·29
3	21 000	21 592	0·038	2·82	450	458·2	0·124	1·82
4	19 500	19 723	0·038	1·14	500	488·2	0·073	−2·36
5	18 000	17 949	0·098	−0·28	650	648·1	0·121	−0·29
6	16 000	16 555	0·080	3·47	550	565·8	0·140	2·87
Average of absolute values			0·062	2·15	—	—	0·114	3·24
Band width = 0–75 Hz								
1	24 000	24 301	0·062	1·25	550	529·1	0·204	−3·80
2	22 000	22 218	0·075	0·99	850	839·6	0·102	−1·22
3	21 000	21 965	0·059	4·60	450	463·3	0·147	2·96
4	19 500	19 607	0·075	0·55	500	522·5	0·153	4·50
5	18 000	18 398	0·109	2·21	650	653·3	0·171	0·51
6	16 000	15 749	0·051	−1·57	550	534·3	0·140	−2·85
Average of absolute values			0·072	1·86	—	—	0·153	2·64

that far exceeds the maximum frequency, no improvement in results is to be expected. This is exemplified by the results of Table II. Based on response time history of 10 000 points contaminated with 1 per cent noise, the mean error and cov for k and c, respectively, are 1·9 per cent and 0·07, and 2·6 per cent and 0·15, for input bandwidth of 75 Hz. The respective maximum values for k are 4·6 per cent and 0·11 and for c are 4·5 per cent and 0·20. There is no improvement compared with the results for the case of bandwidth 50 Hz. However, the results based on input frequency bandwidths of 10 and 25 Hz are significantly inferior.

Table III. Effect of noise in the response data on k and c for input excitation with frequency band 0–50 Hz and sampling length of 10 000 points based on displacement observation

Parameters	Stiffness, k				Damping, c			
Storey no.	Actual value	Mean predicted	cov	Per cent error in mean	Actual value	Mean predicted	cov	Per cent error in mean
Noise intensity = 1 per cent								
1	24 000	24 369	0·066	1·54	550	507·1	0·143	−7·80
2	22 000	21 204	0·050	−3·62	850	813·5	0·085	−4·29
3	21 000	21 592	0·038	2·82	450	458·2	0·124	1·82
4	19 500	19 723	0·038	1·14	500	488·2	0·073	−2·36
5	18 000	17 949	0·098	−0·28	650	648·1	0·121	−0·29
6	16 000	16 555	0·080	3·47	550	565·8	0·140	2·87
Average of absolute values			0·062	2·15	—	—	0·114	3·24
Noise intensity = 3 per cent								
1	24 000	24 923	0·063	3·85	550	544·7	0·178	−0·96
2	22 000	23 223	0·103	5·56	850	906·2	0·093	6·61
3	21 000	20 578	0·085	−2·01	450	435·8	0·194	−3·16
4	19 500	20 821	0·121	6·77	500	522·4	0·150	4·48
5	18 000	18 708	0·189	3·93	650	655·5	0·185	0·85
6	16 000	16 849	0·101	5·31	550	597·1	0·161	8·56
Average of absolute values			0·110	4·57	—	—	0·160	4·10
Noise intensity = 5 per cent								
1	24 000	24 143	0·128	0·60	550	499·8	0·288	−9·13
2	22 000	22 028	0·159	0·13	850	856·1	0·197	0·72
3	21 000	23 155	0·172	10·26	450	521·9	0·228	15·98
4	19 500	20 069	0·129	2·92	500	512·0	0·215	2·40
5	18 000	22 736	0·234	26·31	650	867·6	0·268	33·48
6	16 000	16 845	0·145	5·28	550	564·7	0·134	2·67
Average of absolute values			0·161	7·58	—	—	0·222	10·73

The contamination of response time histories by noises can affect the identification results significantly. As depicted in Table III, the mean error in k increases from 2 to 8 per cent and corresponding cov increases from 0·06 to 0·16 when the noise intensity increases from 1 to 5 per cent. The results for individual storeys can be significantly worse, as in the fifth storey where the mean error in k is 26 per cent with cov of 0·23 for 5 per cent contamination. The same conclusion can be drawn for c.

As an indication of the CPU time taken, identification using a time history of 10 000 points at 0·05 s interval requires about 70 s on the HP 712/60 workstation.

Example 2

To demonstrate the applicability of the algorithm for larger problems, a fifteen-storey shear building where the values of the actual mass are assumed to be 0·25 per cent of the stiffness values and a proportional damping matrix at 1 per cent of the stiffness values, is used. The actual k_i and

Table IV. Effect of bandwidth on k and c of Example 2 for response data with 1 per cent noise and sampling length of 10 000 points based on displacement observation

Parameters	Stiffness, k				Damping, c			
Storey no.	Actual value	Mean predicted	cov	Per cent error in mean	Actual value	Mean predicted	cov	Per cent error in mean
Band width = 0–50 Hz								
1	44 300	45 108	0·045	1·82	443	529·8	0·143	19·59
2	44 300	45 279	0·029	2·21	443	462·0	0·116	4·29
3	30 700	31 713	0·036	3·30	307	340·9	0·069	11·04
4	30 700	31 424	0·023	2·36	307	332·6	0·077	8·34
5	28 000	28 753	0·022	2·69	280	314·2	0·168	12·21
6	28 000	28 475	0·024	1·70	280	302·8	0·108	8·14
7	28 000	28 797	0·029	2·85	280	315·5	0·082	12·68
8	28 000	28 530	0·041	1·89	280	315·6	0·110	12·71
9	28 000	28 658	0·032	2·35	280	298·8	0·125	6·71
10	28 000	28 433	0·042	1·55	280	311·3	0·071	11·18
11	28 000	28 740	0·033	2·64	280	300·0	0·087	7·14
12	26 000	26 999	0·034	3·84	260	311·9	0·122	19·96
13	26 000	26 497	0·038	1·91	260	282·8	0·137	8·77
14	22 000	22 355	0·036	1·61	220	237·4	0·087	7·91
15	22 000	22 764	0·025	3·47	220	247·6	0·091	12·55
Average of absolute values			0·033	2·41	—	—	0·106	10·88
Band width = 0–75 Hz								
1	44 300	44 827	0·045	1·19	443	486·4	0·180	9·80
2	44 300	44 690	0·028	0·88	443	424·3	0·128	−4·22
3	30 700	31 366	0·036	2·17	307	315·8	0·072	2·87
4	30 700	30 965	0·022	0·86	307	304·0	0·085	−0·98
5	28 000	28 323	0·023	1·15	280	287·0	0·182	2·50
6	28 000	28 083	0·026	0·30	280	279·5	0·123	−0·18
7	28 000	28 458	0·030	1·64	280	292·6	0·080	4·50
8	28 000	28 109	0·043	0·39	280	289·3	0·097	3·32
9	28 000	28 282	0·031	1·01	280	273·2	0·124	−2·43
10	28 000	28 003	0·043	0·01	280	285·1	0·075	1·82
11	28 000	28 350	0·033	1·25	280	276·1	0·097	−1·39
12	26 000	26 658	0·036	2·53	260	289·3	0·133	11·27
13	26 000	26 185	0·036	0·71	260	262·3	0·145	0·88
14	22 000	22 054	0·036	0·25	220	218·8	0·092	−0·55
15	22 000	22 562	0·025	2·55	220	230·4	0·094	4·73
Average of absolute values			0·033	1·13	—	—	0·114	3·43

c_i are given in Table IV. The highest structural frequency is 39·62 rad/s. For simulating the data, a sampling rate of 200 points per second over a duration of 50 s is used and two input frequency bandwidths are studied, namely, 50 and 75 Hz. The results are given in Table IV and Figure. 3.

Compared to Example 1, the results are better for both k and c (mean as well as cov) despite the significantly larger degrees of freedom. Both input bandwidths of 50 and 75 Hz produces good results for k (mean error of 2·4 and 1·1 per cent, respectively) as it could excite all the structural

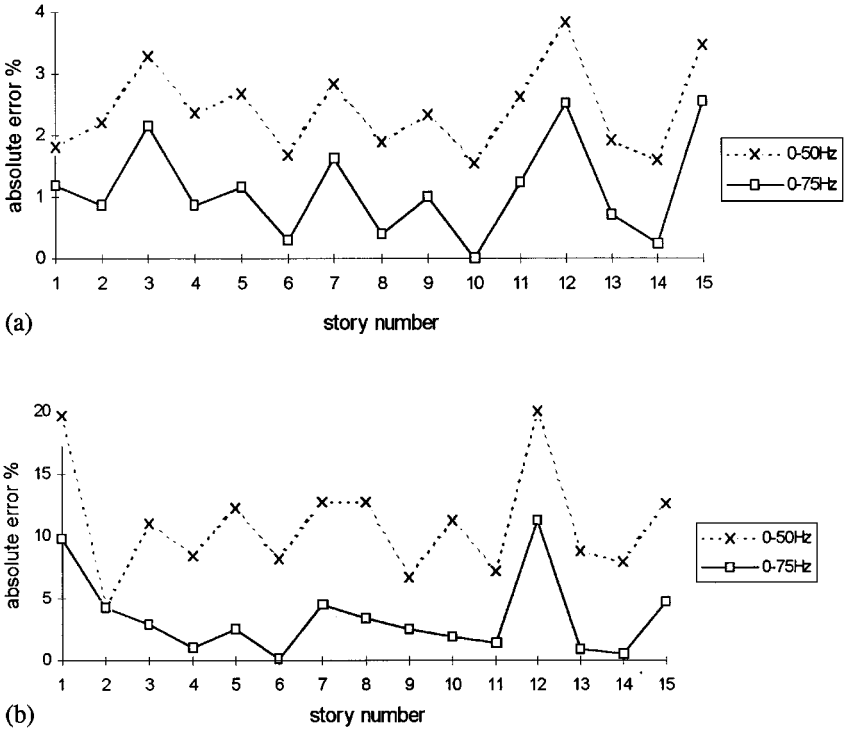

Figure 3. (a) Effect of bandwidth on k for Example 2 with displacement response data having 1 per cent noise and sampling length of 10 000 points. (b) effect of bandwidth on c for Example 2 with displacement response data having 1 per cent noise and sampling length of 10 000 points

modes, although for c the 75 Hz produces better results (see Figure 3). For larger degrees of freedom structures, the Kalman gain matrix is of larger order and can therefore better describe the non-white characteristic of the excitation. This is explained by the fact that as the size of matrix B in equation (4) gets larger, the larger number of combinatorial terms to describe the noise provides a higher degree to better describe its characteristics. This possibly explains the more accurate results comparing with the six DOF example. Therefore, this algorithm is especially effective for MDOF structures.

Example 3

To investigate the accuracy of the algorithm for the case of velocity response data in identification, the fifteen-storey building of Example 2 is considered. The results for input frequency bandwidths of 50 and 75 Hz with velocity time histories of 10 000 sampling points and 1 per cent noise contamination are tabulated in Table V. The overall mean and cov of the error in k and c are comparable with the results of Example 2, indicating that the algorithm is likely to be equally applicable for both displacement and velocity response data. In terms of computation time, identification based on 10 000 time steps takes about 7 min on the HP 712/60 workstation.

Table V. Effect of bandwidth on k and c of Example 3 for response data with 1 per cent noise and sampling length of 10 000 points based on velocity observation

Parameters	Stiffness, k				Damping, c			
Storey no.	Actual value	Mean predicted	cov	Per cent error in mean	Actual value	Mean predicted	cov	Per cent error in mean
Band width = 0–50 Hz								
1	44 300	43 092	0·055	−2·73	443	503·0	0·148	13·53
2	44 300	45 454	0·041	2·61	443	442·4	0·086	−0·13
3	30 700	31 372	0·038	2·19	307	324·1	0·088	5·56
4	30 700	30 908	0·023	0·68	307	322·4	0·092	5·03
5	28 000	29 052	0·046	3·76	280	299·6	0·115	7·01
6	28 000	28 824	0·030	2·94	280	299·6	0·083	7·00
7	28 000	28 645	0·056	2·30	280	285·7	0·108	2·05
8	28 000	28 246	0·058	0·88	280	296·2	0·091	5·78
9	28 000	28 002	0·046	0·01	280	284·9	0·128	1·76
10	28 000	28 015	0·047	0·05	280	291·3	0·144	4·03
11	28 000	29 091	0·042	3·90	280	273·8	0·083	−2·23
12	26 000	27 024	0·037	3·94	260	290·8	0·102	11·83
13	26 000	25 986	0·043	−0·06	260	258·2	0·146	−0·70
14	22 000	22 596	0·036	2·71	220	244·7	0·112	11·24
15	22 000	22 454	0·015	2·06	220	245·1	0·091	11·39
Average of absolute values			0·041	2·05	—	—	0·108	5·95
Band width = 0–75 Hz								
1	44 300	43 787	0·057	−1·16	443	459·3	0·172	3·68
2	44 300	45 677	0·041	3·11	443	423·1	0·096	−4·49
3	30 700	31 494	0·040	2·59	307	318·8	0·083	3·85
4	30 700	31 012	0·024	1·02	307	319·3	0·075	4·00
5	28 000	29 155	0·047	4·13	280	299·2	0·122	6·85
6	28 000	28 887	0·030	3·17	280	297·2	0·089	6·14
7	28 000	28 645	0·055	2·30	280	283·5	0·084	1·24
8	28 000	28 296	0·057	1·06	280	295·4	0·098	5·49
9	28 000	28 032	0·046	0·11	280	285·0	0·113	1·78
10	28 000	28 054	0·048	0·19	280	288·8	0·149	3·14
11	28 000	29 109	0·043	3·96	280	275·7	0·096	−1·52
12	26 000	27 110	0·041	4·27	260	290·2	0·100	11·63
13	26 000	26 032	0·042	0·12	260	264·0	0·136	1·53
14	22 000	22 619	0·038	2·81	220	247·2	0·116	12·38
15	22 000	22 448	0·017	2·03	220	245·8	0·088	11·71
Average of absolute values			0·042	2·14	—	—	0·108	5·30

CONCLUSIONS

From the numerical examples, it can be seen that the Eigenspace Algorithm produces reasonably good results especially for problems with large degrees of freedom. The input frequency bandwidth should preferably be wide enough to excite all the modes of the system and the response time history used in the identification be sufficiently long. The quality of the results is affected by

the level of noise intensity in the observed data. The algorithm is equally applicable for both displacement and velocity response data. The advantages of the EA are its non-iterative nature, the use of well-developed and efficient QR and QSVD techniques, and that it is a self-start scheme requiring no initial guess.

This study is by no means exhaustive. Further work on this algorithm is currently being addressed to widen its applicability. Firstly, the problem of identifying system parameter with unknown input excitation is already not simple and large noise contamination may render the measured response too inaccurate for identification purposes. To extend EA to yield good results for the latter case can be a formidable task. Secondly, the additional problem of missing information in the measured response is a realistic problem that warrants serious study.

Thirdly, the use of acceleration data is not addressed in this study as using the same formulation results in near perfect correlation between the input and observation noise causing numerical difficulties in the algorithm.

APPENDIX. SIMILARITY TRANSFORMATION TO CANONICAL FORM

Let the non-singular transformation matrix T_1 be given by

$$T_1 = \begin{bmatrix} D \\ DA \end{bmatrix}^{-1} = [Q_1\ Q_2] \tag{A.1}$$

such that $T_1^{-1}T_1$ is an identity matrix. This implies that

$$DQ_1 = I_{m\times m} \quad DAQ_1 = 0_{m\times m} \quad DQ_2 = 0_{m\times m} \quad DAQ_2 = I_{m\times m} \tag{A.2}$$

Applying the transformation matrix to D and A results in the OCF as follows:

$$\begin{aligned} D_c &= DT_1 = D[Q_1\ Q_2] = [I_{m\times m}\ 0_{m\times m}] \\ A_c &= T_1^{-1}AT_1 = \begin{bmatrix} D \\ DA \end{bmatrix} A[Q_1\ Q_2] = \begin{bmatrix} 0_{m\times m} & I_{m\times m} \\ DA^2Q_1 & DA^2Q_2 \end{bmatrix} \end{aligned} \tag{A.3}$$

For the case of velocity observation, D_c in the observation equation of the state-space model is $[0_{m\times m}\ I_{m\times m}]$. Applying similarity transformation yields

$$T_v = \begin{bmatrix} D_c \\ D_cA_c \end{bmatrix}^{-1} = A_c^{-1}, \quad D_v = D_cT_v = [I_{m\times m}\ 0_{m\times m}], \quad T_v^{-1}A_cT_v = A_c \tag{A.4}$$

This reduces to the OCF of displacement observation. The solution procedure thus follows that of displacement observation.

REFERENCES

1. V. C. Matzen, 'Time domain identification of linear structures', in H. G. Natke and J. T. P. Yao (eds), *Proc. of Workshop on Struct. Safety Evaluation Based in System Identification Approaches*, Vieweg-Verlag, Braunschweig, 1988.
2. C. B. Lin, T. T. Soong and H. G. Natke, 'Real time system identification of degrading structures', *J. Engng. Mech. ASCE* **116**(10), 2258–2274 (1990).
3. K. D. Hjelmstad, M. R. Banan and M. R. Banan, 'Time domain parameter estimation algorithm for structures. I: computational aspects', *J. Engng. Mech.*, ASCE **121**(3), 424–434 (1995).
4. M. H. A. Davis and R. B. Vinter, *Stochastic Modelling And Control*, Champman & Hall, London, 1985.

5. P. C. Young, 'An instrumental variable method for real-time identification of a noisy process', *Automatica* **6**, 271–287 (1970).
6. M. Shinozuka, C. B. Yun and H. Imai, 'Identification of linear structural dynamic system', *J. Engng. Mech. ASCE* **108**(6), 1371–1390 (1982).
7. H. Imai, C. B. Yun, O. Maruyama and M. Shinozuka, 'Fundamentals of system identification in structural dynamics', *Probab. Engng. Mech.* **4**(4), 162–173 (1989).
8. M. Hoshiya and E. Saito, 'Structural identification by extended Kalman filter', *J. Engng. Mech. ASCE* **110**(12), 1757–1770 (1984).
9. C. G. Koh, L. M. See and T. Balendra, 'Estimation of structural parameters in time domain: a substructure approach', *Earth. Engng. Struct. Dyn.* **20**(8), 787–801 (1991).
10. R. Ghanem and M. Shinozuka, 'Structural system identification I: theory', *J. Engng. Mech. ASCE* **121**(2), 255–264 (1995).
11. M. A. M. Torkamani and A. K. Ahmadi, 'Stiffness identification of a tall building during construction period using ambient tests', *Earth. Engng. Struct. Dyn.* **16**, 1177–1188 (1988).
12. M. Shinozuka, R. Vaicaitis and H. Acada, 'Digital generation of random forces for large-scale experiments', *J. Aircraft* **13**(6), 425–431 (1976).
13. E. Simiu and R. H. Scanlan, *Wind Effects On Structures*, 2nd edn., Wiley, New York, 1986.
14. D. Wang, and A. Halder, 'Element-level system identification with unknown input', *J. Engng. Mech. ASCE* **120**(1), 159–176 (1994).
15. M. S. Ahmed, 'Fast GLS algorithm for parameter estimation', *Automatica* **20**, 231–236 (1984).
16. N. P. Jones, T. Shi, J. H. Ellis and R. H. Scanlan, 'System-identification procedure for system and input parameters in ambient vibration surveys', *J. Wind Engng. Indust. Aerodyn.* **54**/**55**, 91–99 (1995).
17. P. Van Overschee and B. De Moor, *Subspace Identification For Linear Systems*: *Theory–Implementation–Applications*, Kluwer Acad. Publishers, Boston, 1996.
18. J. N. Juang and R. S. Pappa, 'An eigensystem realization algorithm for modal parameter identification and model reduction', *J. Guidance, Control Dyn.* **8**(5), 620–627 (1985).
19. D. J. Inman, *Vibration*: *With Control, Measurement, And Stability*, Prentice-Hall, Englewood Cliffs, NJ, 1989.
20. P. Van Overschee and B. De Moor, 'Subspace algorithms for the stochastic identification problem', *Automatica* **29**(3), 649–660 (1993).

